

# Longitudinal spin dynamics in ferrimagnets: Multiple spin wave nature of longitudinal spin excitations

V. N. Krivoruchko

*Donetsk Institute for Physics and Engineering, NAS of Ukraine, 46, Nauki Avenue, 03680, Kiev, Ukraine*

(Received 19 May 2016; revised manuscript received 30 July 2016; published 30 August 2016)

Motivated by the existing controversy about the physical mechanisms that govern longitudinal magnetization dynamics under the effect of ultrafast laser pulses, in this paper we study the microscopic model of longitudinal spin excitations in a two-sublattice ferrimagnet using the diagrammatic technique for spin operators. The diagrammatic approach provides us with an efficient procedure to derive graphical representations for perturbation expansion series for different spin Green's functions and thus to overcome limitations typical for phenomenological approaches. The infinite series involving all distinct loops built from spin wave propagators are summed up. These result in an expression for the longitudinal spin susceptibility  $\chi^{zz}(\mathbf{q}, \omega)$  applicable in all regions of frequency  $\omega$  and wave vector  $\mathbf{q}$  space beyond the hydrodynamical and critical regimes. A strong renormalization of the longitudinal spin oscillations due to processes of virtual creation and annihilation of transverse spin waves has been found. We have shown that the spectrum of longitudinal excitations consists of a quasirelaxation mode forming a central peak in  $\chi^{zz}(\mathbf{q}, \omega)$  and two (acoustic and exchange) precessionlike modes. As the main result, it is predicted that both acoustic and exchange longitudinal excitations are energetically above similar modes of transverse spin waves at the same temperature and wave vector. The existence of the exchange longitudinal mode at such frequencies can result in a new form of excitation behavior in ferrimagnetic system, which could be important for understanding the physics of nonequilibrium magnetic dynamics under the effect of ultrafast laser pulses in multisublattice magnetic materials.

DOI: [10.1103/PhysRevB.94.054434](https://doi.org/10.1103/PhysRevB.94.054434)

## I. INTRODUCTION

Ultrafast laser-induced magnetic switching in ferrimagnets has become a hot topic of modern magnetism. Uncovering the physical mechanisms that govern ultrafast spin dynamics is critical for understanding fundamental limits of ultrafast spin-based electronics. It is of fundamental importance to realize the time evolution of magnetic moments at high temperatures and time scales approaching femtoseconds. A recent review on the state of the art of ultrafast spin dynamics and its prospects is given by Kirilyuk *et al.* [1].

Ultrafast magnetization dynamics induced by femtosecond laser pulses have been investigated in different ferrimagnetic alloys [2–9]. Several hypotheses have been put forward to explain the observed magnetization switching: the crossing of the angular momentum compensation point [3] and the inverse Faraday effect [2] and its combination with ultrafast heating [4], among others [5,10,11]. The first attempts to describe longitudinal magnetization dynamics in two-sublattice systems have been proposed recently in Refs. [12–17]. It has been shown that spin dynamics simulations within the phenomenological Landau-Lifshitz-Bloch [12–14], Landau-Lifshitz-Gilbert [15], or Landau-Lifshitz-Baryakhtar formulations [6,16,17] can be used to describe ultrafast laser-induced demagnetization in multisublattice magnets when a sufficiently large and fast dissipation of spin angular momentum is assumed.

However, in spite of the progress in phenomenological description, to achieve an exhaustive theoretical explanation of ultrafast magnetization dynamics, first-principles calculations based on quantum-mechanical theory are indispensable. In particular, at present it is commonly accepted that the short time scale of the laser pulse and high temperatures following the excitation lead to processes where longitudinal magnetiza-

tion dynamics becomes pronounced [18]. Naturally, any model of an ultrafast magnetization switching should correctly reproduce equilibrium longitudinal dynamics of the system in the limit of a long-time evolution. Surprisingly enough, whereas dynamics of transverse spin components in multisublattice magnets is well understood theoretically, distinctive features of longitudinal dynamics are still a puzzling point even in the system equilibrium state. Dynamics of longitudinal spin components implies a different physical picture than transverse spin oscillations and poses specific theoretical problems. In fact, this is a very important fundamental question that has not been addressed theoretically to date. Obviously, in-depth knowledge of the physics of longitudinal spin dynamics can shed light on the role of the exchange interaction in the ultrafast dynamics of spin subsystems in complex materials [1].

Note that according to the first publications on this issue [19,20], the longitudinal spin mode arises because of a virtual process of coherent creation and annihilation of ordinary spin waves. In more recent studies based on a diagrammatic approach for spin operators [21], for a ferromagnet the longitudinal excitations have been found at frequencies  $\omega(\mathbf{q}) = [\varepsilon(\mathbf{k}) - \varepsilon(\mathbf{k} \pm \mathbf{q})]$  and have been interpreted in terms of processes of creation and annihilation of two transverse spin waves with energies  $\varepsilon(\mathbf{k})$  and  $\varepsilon(\mathbf{k} \pm \mathbf{q})$  (here the wave vector  $\mathbf{k}$  is a variable). The excitation processes are controlled, however, by the occupation factor, determined through the Bose distribution function  $n(\varepsilon(\mathbf{k}))$ , which makes the spin waves with  $\mathbf{k} \sim 0$  the dominant ones.

Whereas the underlying magnetization dynamics of multisublattice magnets has become a hot topic at present, complete understanding of this phenomenon in ferrimagnets is still missing. In the present paper, a basic understanding of the longitudinal spin dynamics in ferrimagnetic materials is addressed. To this end, we used a general theoretical treatment

aiming to overcome limitations of the models [6,12–17] and to reveal a unique physical picture common to different multisublattice magnets. Namely, we consider the microscopic Heisenberg model of a two-sublattice ferrimagnet. The convenient version of the diagrammatic technique for spin operators has been used to provide quantitative calculation of magnetization excitation frequencies and relaxation times. A detailed account of this diagrammatic technique is given in the textbooks [22,23].

We start in the next section with the formulation of a simple model for a two-sublattice ferrimagnet. In Sec. III, a diagrammatic representation of the longitudinal spin Green's functions (GFs) is formulated. Since, as expected, the quantum dynamics of longitudinal spin components is generated by virtual processes of creation and annihilation of spin waves, the mathematical problem reduces to summing up all the loop diagrams describing these processes. The complexity of the problem arises from the fact that a commutator of two spin operators is not a  $c$  number. Therefore, the series of the loop diagrams turns out to be rather complicated and contains four different types of loops. To sum up these series, we use a method called generalized random-phase approximation (RPA) elaborated on earlier (see [24,25]). By summing up all one- and two-loop diagrams in Sec. IV, we arrive at an expression for the longitudinal GF, the denominator of which includes all terms of  $1/z$  order ( $z$  is the first coordination number of a relevant magnetic lattice). Analytic continuation of the Matsubara-type spin GFs onto the real-frequency axis determines the longitudinal susceptibility  $\chi^{zz}(\mathbf{q}, \omega)$  of the ferrimagnet. The susceptibility is examined as a function of frequency  $\omega$  and wave vector  $\mathbf{q}$ . This analysis shows that the dynamics of longitudinal spin components corresponds to a few virtual processes of creation and annihilation of transverse spin waves. The dynamics was studied and discussed in detail within an approximation of a quadratic spin wave dispersion law. The last section summarizes our main results. Some cumbersome mathematical details are expounded in Appendices A–C.

## II. THE MODEL

To capture the main physics, we consider the simple isotropic model for a two-sublattice ferrimagnet. In the absence of any external influences, the atomistic spin model is described purely by exchange interactions, given by the Heisenberg Hamiltonian:

$$H = \sum_{\mathbf{f}, \mathbf{g}} J_{\mathbf{fg}} \left[ \frac{1}{2} (S_{1\mathbf{f}}^+ S_{2\mathbf{g}}^- + S_{1\mathbf{f}}^- S_{2\mathbf{g}}^+) + S_{1\mathbf{f}}^z S_{2\mathbf{g}}^z \right]. \quad (1)$$

Here  $\mathbf{S}_{1\mathbf{f}}$  and  $\mathbf{S}_{2\mathbf{g}}$  are the spin operators on an  $\mathbf{f}$ th and  $\mathbf{g}$ th sites of sublattices 1 and 2, respectively, and the circular spin operators are definite as usual,  $S^\pm = (S^x \pm S^y)$ ;  $J_{\mathbf{fg}}$  stands for the exchange integral between spins. We will suggest that  $S_1 > S_2$  and  $J_{\mathbf{fg}} > 0$ , i.e., the sublattices, are in antiparallel orientation.

We rewrite the Hamiltonian (1) in the form  $H = E_0 + H_0 + H_{\text{int}}$ . Here  $E_0 = -J_0 S_1 S_2 N$  is the ground-state energy ( $N$  is the number of magnetic unit cells);  $H_0$  stands

for the Hamiltonian of the molecular field of a standard structure:

$$H_0 = -y \sum_{\mathbf{f}} S_{1\mathbf{f}}^z - x \sum_{\mathbf{g}} S_{2\mathbf{g}}^z, \quad (2a)$$

where  $y = \langle S_2^z \rangle J_0$ ,  $x = \langle S_1^z \rangle J_0$  and  $J_0 = J_{\mathbf{q}=0}$  is the Fourier transform of the exchange interaction. The interaction Hamiltonian  $H_{\text{int}}$  is of the form

$$H_{\text{int}} = \sum_{\mathbf{f}, \mathbf{g}} J_{\mathbf{fg}} \left[ \frac{1}{2} (S_{1\mathbf{f}}^+ S_{2\mathbf{g}}^- + S_{1\mathbf{f}}^- S_{2\mathbf{g}}^+) + (S_{1\mathbf{f}}^z - \langle S_1^z \rangle) (S_{2\mathbf{g}}^z - \langle S_2^z \rangle) \right]. \quad (2b)$$

In the zeroth-order approximation of a self-consistent field we have  $\langle S_1^z \rangle^{(0)} = b_1(\beta y_0 S_1)$ ,  $\langle S_2^z \rangle^{(0)} = b_2(\beta x_0 S_2)$ ,  $b(z) = S B_S(z)$ , where  $B_S(z)$  stands for the Brillouin function,  $y_0 = b_2 J_0$ ,  $x_0 = b_1 J_0$ , and  $\beta^{-1} = T$  is temperature. In an antiferromagnetic ground state, the mean value of a magnetic unit-cell magnetization is equal to  $M = \mu_B (g_1 b_1 - g_2 b_2)$ , where  $\mu_B$  is the Bohr magneton and  $g_{1(2)}$  stands for the  $g$  factor of the sublattices.

As is known [22,23,25], within the microscopic (Green's function method) approach, the study of a system's longitudinal magnetization dynamics is based on the dynamic susceptibility  $\chi^{zz}(\mathbf{q}, \omega)$  calculation as a function of frequency  $\omega$  and momentum  $\mathbf{q}$ , which in turn is reduced to the retarded spin GFs calculation:  $\chi^{zz}(\mathbf{q}, \omega) \rightarrow G^{(R)}(\mathbf{q}, \omega)$ . In our case, the calculation of the system's longitudinal susceptibility  $\chi^{zz}(\mathbf{q}, \omega)$  corresponds to the calculation of the retarded longitudinal spin GF  $G_{\text{tot}}^{zz(R)}(\mathbf{q}, \omega)$ :

$$\begin{aligned} \chi^{zz}(\mathbf{q}, \omega) &= \langle\langle \widehat{T} M_{\text{tot}}^z(t) | M_{\text{tot}}^z(0) \rangle\rangle_{\mathbf{q}, \omega} \\ &= -\frac{\mu_B^2}{v_0} G_{\text{tot}}^{zz(R)}(\mathbf{q}, \omega). \end{aligned} \quad (3)$$

Here  $M_{\text{tot}}^z$  is a  $z$  component of the total magnetization  $\mathbf{M}_{\text{tot}} = \mu_B (g_1 \mathbf{S}_1 + g_2 \mathbf{S}_2)$ , and  $v_0$  stands for the volume of a primitive magnetic cell. The symbol  $\langle\langle \dots \rangle\rangle_{\mathbf{q}, \omega}$  denotes the Fourier transform of the trace of  $\rho_0(\dots)$ , with  $\rho_0 = \exp(-\beta H_0) / Sp[\exp(-\beta H_0)]$ ;  $\widehat{T}$  stands for the time-ordering operator. There are theorems proving that the poles of the retarded GFs correspond to the natural frequencies of magnetization excitations that are transverse magnetization oscillations of the spins or ordinary spin waves and longitudinal spin oscillations. In turn, the retarded GFs of the system can be obtained from the temperature GFs by analytic continuation from the Matsubara frequencies  $i\omega_n$  onto the real axis  $i\omega_n \rightarrow \omega + i\delta$ , ( $\delta \rightarrow 0$ ) (for more details, see, e.g., [22,23,25]).

In our case of a two-sublattice system, the total GF  $G_{\text{tot}}^{zz(R)}(\mathbf{q}, \omega)$  can be reduced to four sublattice longitudinal GFs  $G_{ij}^{zz}(\mathbf{q}, i\omega_n)$  ( $i, j = 1, 2$ ) as follows:

$$\begin{aligned} G_{\text{tot}}^{zz}(\mathbf{q}, i\omega_n) &= G_{\text{tot}}^{zz}(q) \\ &= \langle\langle \widehat{T} (g_1 \delta S_1^z - g_2 \delta S_2^z) | (g_1 \delta S_1^z - g_2 \delta S_2^z) \rangle\rangle \\ &= g_1^2 G_{11}^{zz}(q) - g_1 g_2 [G_{12}^{zz}(q) + G_{21}^{zz}(q)] \\ &\quad + g_2^2 G_{22}^{zz}(q), \end{aligned} \quad (4)$$

where  $\delta S_i^z = S_i^z - \langle S_i^z \rangle$  and  $G_{ij}^{zz} = \langle \langle \widehat{T} \delta S_i^z | \delta S_j^z \rangle \rangle$ . Here and below we use the notation  $q = \{\mathbf{q}, i\omega_n\}$ , where  $\mathbf{q}$  stands for the momentum and the Matsubara frequency  $i\omega_n = i2\pi nT$  ( $n = 0, \pm 1, \pm 2, \dots$ ). Thus, the calculation of the dynamic susceptibility  $\chi^{zz}(\mathbf{q}, \omega)$  reduces to the calculation of the sublattice longitudinal GFs  $G_{ij}^{zz}(\mathbf{q}, i\omega_n)$ .

### III. GREEN'S FUNCTIONS OF LONGITUDINAL SPIN COMPONENTS

To calculate the sublattice GFs we use the Larkin equation derived earlier in the framework of the diagrammatic technique for spin operators. Without dwelling on the details of summing up the diagram series (Refs. [22,23,25] contain technical details concerning the construction of the spin diagram technique for the Heisenberg magnet), we present here the final analytic results. One can show that the graph series for the  $G_{ij}^{zz}(q)$  functions of a two-sublattice ferrimagnet can be presented analytically in the form

$$G_{11}^{zz}(q) = \Sigma_{11}^z(q) \{ [1 - J_{\mathbf{q}} \Sigma_{12}^z(q)] [1 - J_{\mathbf{q}} \Sigma_{21}^z(q)] - J_{\mathbf{q}}^2 \Sigma_{11}^z(q) \Sigma_{22}^z(q) \}^{-1} \quad (5)$$

for  $G_{11}^{zz}(q)$  and

$$G_{21}^{zz}(q) = \{ [1 - J_{\mathbf{q}} \Sigma_{12}^z(q)] \Sigma_{21}^z(q) + J_{\mathbf{q}} \Sigma_{11}^z(q) \Sigma_{22}^z(q) \} \times \{ [1 - J_{\mathbf{q}} \Sigma_{12}^z(q)] [1 - J_{\mathbf{q}} \Sigma_{21}^z(q)] - J_{\mathbf{q}}^2 \Sigma_{11}^z(q) \Sigma_{22}^z(q) \}^{-1} \quad (6)$$

for  $G_{21}^{zz}(q)$ . One can obtain expressions for the functions  $G_{22}^{zz}(q)$  and  $G_{12}^{zz}(q)$  from Eqs. (5) and (6), respectively, by substituting  $1 \rightarrow 2 \rightarrow 1$ . In terms of the diagrammatic technique, the quantity  $\Sigma_{ij}^z(q)$  is called the irreducible (by Larkin's method of isolating the irreducible diagrams) parts. Note that the irreducibility is understood here in the sense that  $\Sigma_{ij}^z(q)$  is represented by the collection of all diagrams from the series for  $G_{ij}^{zz}(q)$  that cannot be cut across a line of interaction  $J_{\mathbf{q}}$ .

Summarizing up the results, for the GF  $G_{\text{tot}}^{zz}(q)$  we obtain the following general expression:

$$G_{\text{tot}}^{zz}(q) = \frac{N(q)}{D(q)}. \quad (7)$$

Here we specify the numerator as

$$N(q) = g_1^2 \Sigma_{11}^z(q) - g_1 g_2 [ \Sigma_{12}^z(q) + \Sigma_{21}^z(q) - 2J_{\mathbf{q}} \Sigma_{12}^z(q) \Sigma_{21}^z(q) + 2J_{\mathbf{q}} \Sigma_{11}^z(q) \Sigma_{22}^z(q) ] + g_2^2 \Sigma_{22}^z(q) \quad (8)$$

and the denominator as

$$D(q) = [1 - J_{\mathbf{q}} \Sigma_{12}^z(q)] [1 - J_{\mathbf{q}} \Sigma_{21}^z(q)] - J_{\mathbf{q}}^2 \Sigma_{11}^z(q) \Sigma_{22}^z(q). \quad (9)$$

By calculating the longitudinal GF irreducible parts  $\Sigma_{ij}^z(q)$  we will use the approximation when all ladder diagrams with antiparallel lines have been summed. Typically, such summing corresponds to the so-called RPA and rather well describes the ground state and dynamics of magnetic systems (see, for example, Refs. [24,25]). This approximation was used,

in particular, by Izyumov *et al.* [21] to study the longitudinal spin dynamics in the Heisenberg ferromagnet.

It can be shown that in the case of the zeroth order of a large interaction radius (or of the zeroth order of the parameter  $1/z$ ) one obtains  $\Sigma_{11}^z(\mathbf{q}, i\omega_n) = \delta_{n,0} b'_1$ ,  $\Sigma_{22}^z(\mathbf{q}, i\omega_n) = \delta_{n,0} b'_2$ ,  $\Sigma_{12}^z(\mathbf{q}, i\omega_n) = \Sigma_{21}^z(\mathbf{q}, i\omega_n) = 0$  (here  $b'$  stands for the first derivative of the Brillouin function and  $\delta_{n,0} = \delta_{\omega_n,0}$  is the Kronecker symbol for the corresponding frequency difference). Within this approximation we get [20]

$$G_{11}^{zz(0)}(\mathbf{q}, i\omega_n) = \frac{b'_1}{1 - (\beta J_{\mathbf{q}})^2 b'_1 b'_2} \delta_{n,0},$$

$$G_{22}^{zz(0)}(\mathbf{q}, i\omega_n) = \frac{b'_2}{1 - (\beta J_{\mathbf{q}})^2 b'_1 b'_2} \delta_{n,0},$$

$$G_{12}^{zz(0)}(\mathbf{q}, i\omega_n) = G_{21}^{zz(0)}(\mathbf{q}, i\omega_n) = \frac{b'_1 b'_2}{1 - (\beta J_{\mathbf{q}})^2 b'_1 b'_2} \delta_{n,0}.$$

Note that within this approximation we deal with *static* fluctuations of the longitudinal spin components, which are characterized by the Brillouin function derivatives and which are responsible for the distinction between the isolated and isothermal susceptibilities of the system (see below). We emphasize in this relation that the traditional representation of spin operators by Bose operators (e.g., the Holstein-Primakov or Dyson-Maleev representations) only accounts for the dynamic fluctuations in the magnetization, i.e., a reduction in the magnetization of the sublattice owing to thermal excitation of spin waves. Static fluctuations of the longitudinal components of the spin are entirely neglected in terms of these representations. This circumstance, in particular, dictates the need to use spin operator diagram techniques in order to correctly describe properties of the systems at finite temperatures. The difference in the nature of Bose and spin operators takes on special significance if we consider magnetic system behavior at high enough temperatures. In this temperature region the basic fact of the difference in the number of states [finite  $(2S+1)$  for spin operator states and an infinite number of states for Bose operators] plays a crucial role already in dynamic.

Temperature renormalization of the spectrum and damping of spin wave excitations owing to the scattering of spin waves on (longitudinal) fluctuations in the magnetization both appear in the first approximation with respect to the reciprocal of the interaction radius. Note that the "standard" damping of spin wave oscillations owing to their scattering on one another occurs only in the next (second) approximation of the perturbation theory. (Spin wave relaxation in rare-earth ferrite garnets has been studied previously [26].) To restore the dynamical characteristics, we need to calculate the irreducible parts  $\Sigma_{ij}^z(q)$  within a high-order approximation.

The graphs for the "uncuttable" parts  $\Sigma_{ij}^z(q)$  of the next order (one-loop order) are shown in Fig. 1. The thick lines represent the "dressed" transverse GFs  $G_{ij}(q) = -1/2 \langle \langle \widehat{T} S_{i\mathbf{g}}^+ | S_{j\mathbf{f}}^- \rangle \rangle |_{\mathbf{q}, \omega}$ , and the open points indicate vertices corresponding to the operators  $S_i^z$  ( $i = 1, 2$ ). The dressed transverse GFs (thick lines) of spin wave lines are a result of the summation graphical series for the transverse GFs in the Hartree-Fock approximation shown in Fig. 2 (here the wavy

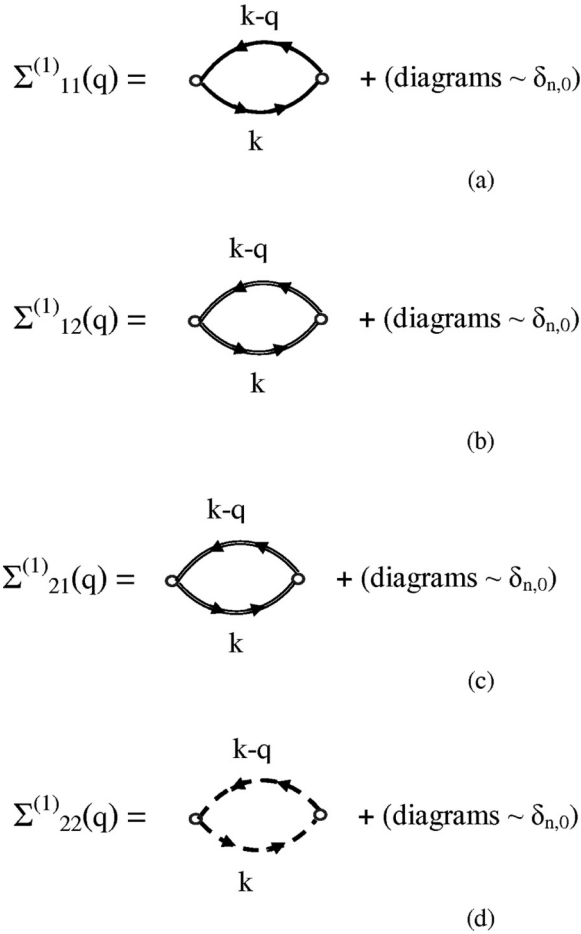


FIG. 1. One-loop order diagrams for irreducible parts of the longitudinal spin Green's functions. Here and in Figs. 2, 3, and 4 external hollow vertices correspond to spin operators  $S_i^z$  ( $i = 1, 2$ ); the thick solid line represents the dressed Green's function  $G_{11}(q)$ ; the thick dashed line describes the dressed Green's function  $G_{22}(q)$ , and the double solid line illustrates the dressed  $G_{12}(q)$  or  $G_{21}(q)$  Green's function. Only the diagrams describing the Kubo susceptibility are shown explicitly.

line is the graphical representation of the interaction  $J_q$ ). The analytical solution of the graphical equations for the transverse GFs is given in Appendix A. In accordance with the rules for the diagram techniques, a block encompassing  $N$  operators  $S^z$  is to be compared to the  $(N - 1)$ th derivative of the function  $b(z)$  of the form  $\sim \delta_{n,0} b^{(N-1)}(z)$ . The analytical expression of these diagrams contains a singular discrete frequency part  $\sim \delta_{n,0}$  and thus does not depend on the thermodynamic time (see Refs. [22,23] for more details). Let us recall here that the singular contribution to the temperature GF arises due to the distinction between the isolated and isothermal susceptibilities of the system [27,28]. As was shown in these studies, the intensity of the singular contribution coincides with the distinction between the isothermal and isolated susceptibilities at the zeroth frequency. In accordance with the general analysis of different susceptibilities [27,28] the distinction between them points to the nonergodicity of the system. We are interested in the Kubo (or isolated) susceptibility of the system derived from the quantity  $G_{\text{tot}}^{zz}(\mathbf{q}, i\omega_n)$  by analytic continuation from

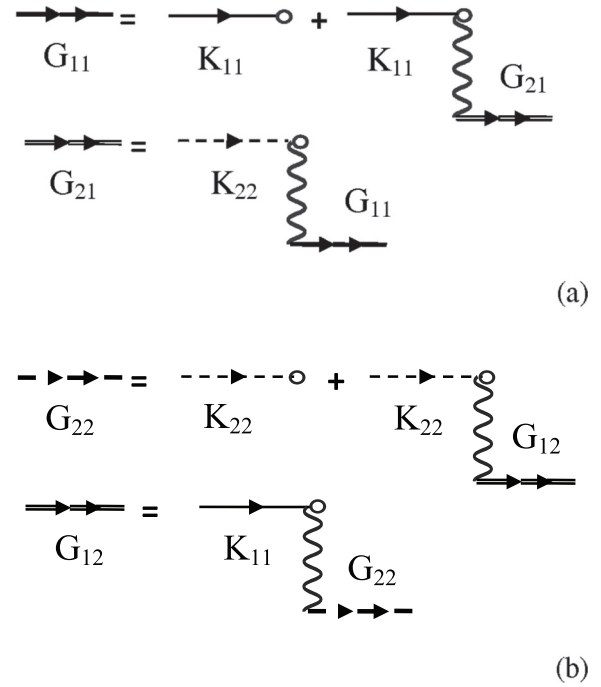


FIG. 2. Graphical representation of the system of equations for dressed transverse (a)  $G_{11}(q)$  and  $G_{21}(q)$  and (b)  $G_{22}(q)$  and  $G_{12}(q)$  Green's functions. The thin solid line represents the undressed (initial) Green's function  $K_{11}(q)$ ; the thin dashed line describes the initial (undressed) Green's function  $K_{22}(q)$ . Here and in Fig. 4 a wavy line corresponds to the interaction  $J_q$ .

the Matsubara frequencies onto the real axis  $i\omega_n \rightarrow \omega + i\delta$  ( $\delta \rightarrow 0$ ). For this reason the diagrams which do not depend on the thermodynamic time (i.e.,  $\sim \delta_{n,0}$ ) in Fig. 1 (and in Fig. 3 below) are not shown.

Returning to the graphs in Fig. 1 and following the rules of the diagram techniques, one can obtain their analytic expressions. For the diagrams in Fig. 1 we write the result in the form  $\Sigma_{11}^z(q) = \Pi(q) + (\sim \delta_{n,0})$ ,  $\Sigma_{12}^z(q) = \Sigma_{21}^z(q) = \Phi(q) + (\sim \delta_{n,0})$ , and  $\Sigma_{22}^z(q) = B(q) + (\sim \delta_{n,0})$ . Here  $(\sim \delta_{n,0})$  stands for the analytic expressions of the diagrams which do not contribute to the isolated system susceptibilities (as already mentioned, these diagrams are not shown in Fig. 1 explicitly). Then the one-loop graph's contribution to the longitudinal GFs is

$$\Pi(q) = N^{-1} \beta^{-1} \sum_p G_{11}(p) G_{11}(p - q), \quad (10)$$

$$\Phi(q) = N^{-1} \beta^{-1} \sum_p G_{12}(p) G_{21}(p - q), \quad (11)$$

$$B(q) = N^{-1} \beta^{-1} \sum_p G_{22}(p) G_{22}(p - q). \quad (12)$$

Explicit expressions for the transversal GFs  $G_{ij}(q)$  are given by Eqs. (A3)–(A5).

All possible two-loop diagrams related to the Kubo (isolated) susceptibility are depicted in Fig. 3. There two external vertices of the GFs (1 and 2) are represented by open points with incoming and outgoing Green's lines. Other arrangements of external vertices do not exist. The hatched squares here represent graphically the effective four-point

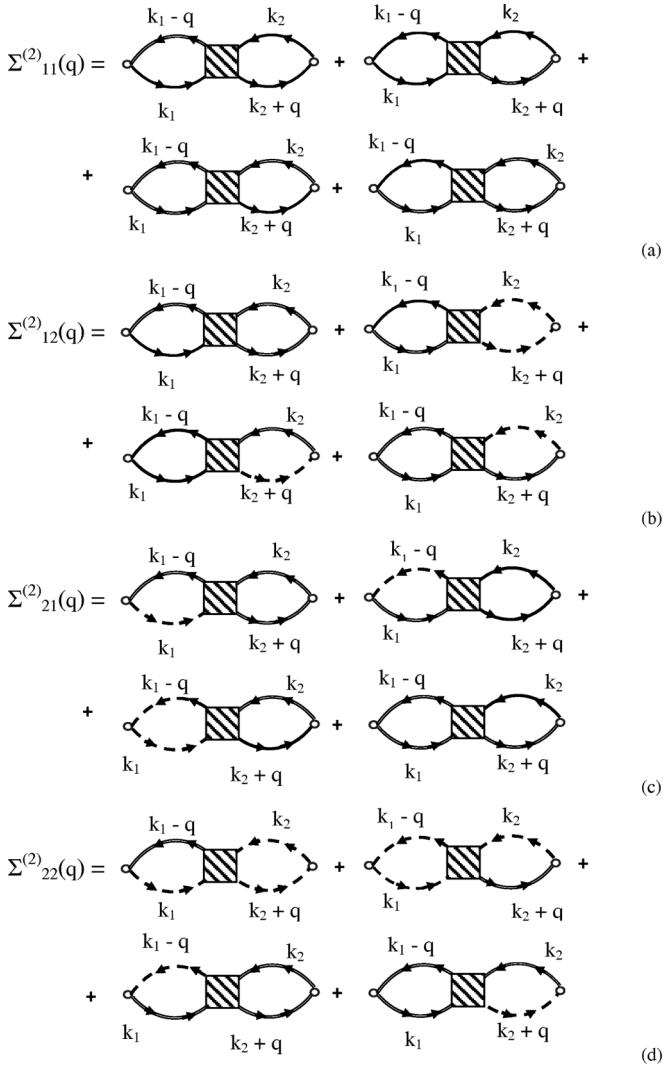


FIG. 3. Two-loop order diagrams for irreducible parts of the longitudinal spin Green's functions. The hatched squares represent graphically the effective four-point vertices  $\Gamma_{ii,ij}(k_1, k_2 | k_1 - q, k_2 + q)$ . Only the diagrams describing the Kubo susceptibility are shown.

vertices  $\Gamma_{ii,ij}(k_1, k_2 | k_1 - q, k_2 + q)$ . The calculation of these vertices is a key point now to proceed further.

The equations for the vertices  $\Gamma_{ii,ij}(k_1, k_2 | k_1 - q, k_2 + q)$  are presented graphically in Fig. 4. Here, as in Fig. 2, the wavy line is the graphical representation of the interaction  $J_q$ . The graphical equation for the vortex  $\Gamma_{11,12}(k_1, k_2 | k_1 - q, k_2 + q)$  shown in Fig. 4(a) corresponds to the analytical expression of the following form:

$$\begin{aligned} \Gamma_{11,12}(k_1, k_2 | k_1 - q, k_2 + q) \\ = J_{k_2+q} + \beta^{-1} N^{-1} \sum_{k_3} J_{k_3+q} G_{11}(k_3) G_{21}(k_3 + q) \\ \times \Gamma_{11,12}(k_3 + q, k_2 | k_3, k_2 + q). \end{aligned}$$

This integral equation can be transformed into an algebraic one. To this end, let us first multiply both sides by  $J_{k_1} G_{11}(k_1 - q) G_{21}(k_1)$  and then sum up over  $k_1$ . This results in a linear

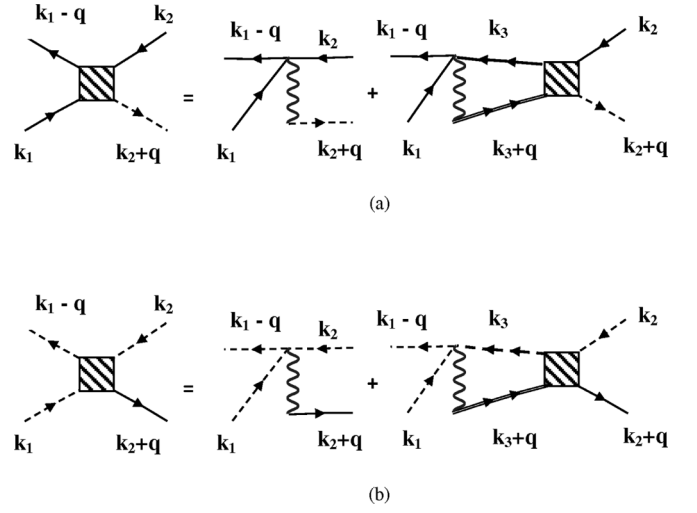


FIG. 4. Graphical representation of the equation for the effective four-point vortex: (a)  $\Gamma_{11,12}(k_1, k_2 | k_1 - q, k_2 + q)$  and (b)  $\Gamma_{22,21}(k_1, k_2 | k_1 - q, k_2 + q)$ .

equation with the solution

$$\Gamma_{11,12}(k_1, k_2 | k_1 - q, k_2 + q) = \frac{J_{k_2+q}}{1 - Q(q)},$$

where

$$Q(q) = N^{-1} \beta^{-1} \sum_p G_{11}(p) G_{21}(p - q). \quad (13)$$

The graphical equation for another vortex  $\Gamma_{22,21}(k_1, k_2 | k_1 - q, k_2 + q)$  shown in Fig. 4(b) leads to the analytical expression

$$\begin{aligned} \Gamma_{22,21}(k_1, k_2 | k_1 - q, k_2 + q) \\ = J_{k_2+q} + \beta^{-1} N^{-1} \sum_{k_3} J_{k_3+q} G_{22}(k_3) G_{12}(k_3 + q) \\ \times \Gamma_{22,21}(k_3 + q, k_2 | k_3, k_2 + q). \end{aligned}$$

This integral equation can also be rewritten in an algebraic form. Like in the previous case, we multiplied both sides of the equation by  $J_{k_1} G_{22}(k_1 - q) G_{12}(k_1)$  and then summed up over  $k_1$ . The solution can be presented as

$$\Gamma_{22,21}(k_1, k_2 | k_1 - q, k_2 + q) = \frac{J_{k_2+q}}{1 - \Lambda(q)},$$

where

$$\Lambda(q) = N^{-1} \beta^{-1} \sum_p G_{22}(p) G_{12}(p - q). \quad (14)$$

Using the obtained expressions for the vertices and summing up all the contributions, we found the following analytic expressions for the two-loop diagrams shown in Fig. 3:

$$\begin{aligned} \Sigma_{11}^{z(2)}(q) &= 2Q(q) \left[ \frac{\Pi(q)}{1 - Q(q)} + \frac{\Phi(q)}{1 - \Lambda(q)} \right], \\ \Sigma_{12}^{z(2)}(q) &= \Sigma_{21}^{z(2)}(q) \\ &= \frac{Q(q)\Phi(q) + \Pi(q)\Lambda(q)}{1 - Q(q)} + \frac{B(q)Q(q) + \Phi(q)\Lambda(q)}{1 - \Lambda(q)}, \\ \Sigma_{22}^{z(2)}(q) &= 2\Lambda(q) \left[ \frac{\Phi(q)}{1 - Q(q)} + \frac{B(q)}{1 - \Lambda(q)} \right]. \end{aligned}$$

The total contribution of the one- and two-loop graphs to the irreducible elements  $\Sigma_{ij}^z(q)$  can be written as follows:

$$\Sigma_{11}^z(q) = \Pi(q) \frac{1 + Q(q)}{1 - Q(q)} + 2 \frac{Q(q)\Phi(q)}{1 - \Lambda(q)}, \quad (15)$$

$$\Sigma_{12}^z(q) = \Sigma_{21}^z(q) = \Phi(q) + \frac{Q(q)\Phi(q) + \Pi(q)\Lambda(q)}{1 - Q(q)} + \frac{B(q)Q(q) + \Phi(q)\Lambda(q)}{1 - \Lambda(q)}, \quad (16)$$

$$\Sigma_{22}^z(q) = B(q) \frac{1 + \Lambda(q)}{1 - \Lambda(q)} + 2 \frac{\Lambda(q)\Phi(q)}{1 - Q(q)}. \quad (17)$$

Thus, to find the isolated (Kubo) susceptibility  $\chi^{zz}(\mathbf{q}, \omega)$  it is necessary to calculate five functions,  $\Pi(q)$ ,  $\Phi(q)$ ,  $B(q)$ ,  $Q(q)$ , and  $\Lambda(q)$ , given by formulas (10)–(14), respectively. After simple but cumbersome calculations, one can obtain the analytical expressions for these functions. They are presented in the explicit form in Appendix B.

$$\Phi(q) = \frac{b_1^2 b_2^2}{N} \sum_{\mathbf{p}} \frac{J_{\mathbf{p}}}{\varepsilon_{1\mathbf{p}} + \varepsilon_{2\mathbf{p}}} \frac{J_{\mathbf{p}-\mathbf{q}}}{\varepsilon_{1\mathbf{p}-\mathbf{q}} + \varepsilon_{2\mathbf{p}-\mathbf{q}}} \times \left\{ \frac{n_1(\varepsilon_{1\mathbf{p}}) - n_1(\varepsilon_{1\mathbf{p}-\mathbf{q}})}{i\omega_q - \varepsilon_{1\mathbf{p}} + \varepsilon_{1\mathbf{p}-\mathbf{q}}} - \frac{n_2(\varepsilon_{2\mathbf{p}}) - n_2(\varepsilon_{2\mathbf{p}-\mathbf{q}})}{i\omega_q + \varepsilon_{2\mathbf{p}} - \varepsilon_{2\mathbf{p}-\mathbf{q}}} + \frac{1 + n_1(\varepsilon_{1\mathbf{p}-\mathbf{q}}) + n_2(\varepsilon_{1\mathbf{p}})}{i\omega_q + \varepsilon_{2\mathbf{p}} + \varepsilon_{1\mathbf{p}-\mathbf{q}}} - \frac{1 + n_1(\varepsilon_{1\mathbf{p}}) + n_2(\varepsilon_{2\mathbf{p}-\mathbf{q}})}{i\omega_q - \varepsilon_{1\mathbf{p}} - \varepsilon_{2\mathbf{p}-\mathbf{q}}} \right\}. \quad (19)$$

[Here and below we introduce the designation  $\varepsilon_i(\mathbf{q}) = \varepsilon_{i\mathbf{q}}$ . The expressions for  $\Pi(q)$  and  $B(q)$ , Eqs. (10) and (12), are represented by Eqs. (B1) and (B2) in Appendix B, and as one can see, they have similar structures.

The analysis of Eq. (19), as well as Eqs. (B1) and (B2), shows that the dynamics of longitudinal spin components is due to a few processes of virtual creation and annihilation of transverse spin wave modes. Namely, the first channel, the first item in the braces on the right-hand side (rhs) of Eq. (19), represents the processes of creation and annihilation of two spin waves with energies  $\varepsilon_{1\mathbf{p}}$  and  $\varepsilon_{1\mathbf{p}-\mathbf{q}}$ , which correspond to in-phase sublattice magnetization precession. This channel is controlled by the occupation factor  $n_1(\varepsilon_{1\mathbf{p}})$ , which makes the spin waves with  $\mathbf{p} \sim 0$  the dominant ones. Simple comparison reveals that this channel is a direct analog of the magnetization longitudinal dynamics in a ferromagnet found by Izyumov *et al.* [21].

There is also the second channel, the second term on the rhs of Eq. (19), with characteristic energy at  $\omega(\mathbf{q}) = \varepsilon_{2\mathbf{p}} - \varepsilon_{2\mathbf{p}-\mathbf{q}}$ . It corresponds to virtual creation and annihilation of exchange spin waves with antiphase precession of sublattice magnetization. This channel is also controlled by the related occupation factor determined through the Bose distribution functions  $n_2(\varepsilon_{2\mathbf{p}})$ , which makes the spin waves with  $\mathbf{p} \sim 0$  the dominant ones.

It is not difficult to see that the last two items in the braces in Eq. (19) present the third channel of longitudinal excitations. Namely, there is a two-spin-wave creation/annihilation process at frequency  $\omega(\mathbf{q}) = \varepsilon_{1\mathbf{p}} + \varepsilon_{2\mathbf{p}-\mathbf{q}}$  which corresponds to creation or annihilation of one acoustic and one exchange transverse mode. This channel remains in force even in the

#### IV. LONGITUDINAL SPIN DYNAMICS IN FERRIMAGNET

The excitation spectrum of the system is determined by the poles of the analytic continuation  $i\omega_n \rightarrow \omega + i\delta$  of the temperature GF  $G_{\text{tot}}^{zz}(\mathbf{q}, i\omega_n)$ . The real part of the pole is the energy of a quasiparticle excitation, while the imaginary part characterizes broadening of the energy level, i.e., a quasiparticle damping. Thus, we should investigate whether the  $G_{\text{tot}}^{zz}(\mathbf{q}, i\omega_n)$  denominator has solutions that would determine the longitudinal wave excitations. To this end, let us examine Eq. (9) more closely. First of all, before proceeding to an estimation of this expression in some limiting cases, let us qualitatively analyze the origin of the longitudinal spin excitations in the system under consideration. It is informative to start with the one-loop order approximation. In this approach the denominator (9) can be rewritten in the form

$$D(q) = [1 - J_{\mathbf{q}}\Phi(q)]^2 - J_{\mathbf{q}}^2 \Pi(q)B(q). \quad (18)$$

After summing up over the discrete Matsubara frequency for the function  $\Phi(q) = \Phi(\mathbf{q}, i\omega_n)$ , Eq. (11), we obtained

absence of thermal excitations, i.e., when  $n_1(\varepsilon_{1\mathbf{p}}) \sim 0$  and/or  $n_2(\varepsilon_{2\mathbf{p}}) \sim 0$ .

All listed mechanisms of the longitudinal spin excitations remain valid in the high-loop approximation, too. Indeed, calculation of the functions  $Q(q)$  and  $\Lambda(q)$  leads us to the final expressions given by Eqs. (B3) and (B4), respectively, in Appendix B. Analyzing these functions, we see that all conclusions made above remain in force. Thus, the structure of the denominator  $D(\mathbf{q}, \omega)$  and, in particular, the equation  $\text{Re}D(\mathbf{q}, \omega) = 0$  that determines the dispersion law point to a strong *renormalization* of longitudinal spin excitation frequency due to a few virtual transverse spin wave creation/annihilation processes. Accordingly, as will be shown below, the energy of longitudinal spin vibration strongly differs from a simple algebraic sum of acoustic and/or exchange mode energy.

Let us now examine Eq. (18) more closely. The main physics can be captured in a long-wave limit ( $ak \ll 1$ ). Within this approximation the energy of transverse spin wave excitations reads [see Eqs. (A6) and (A7)]

$$\varepsilon_{1\mathbf{k}} = D(ak)^2, \quad D = 2 \frac{b_1 b_2}{b_1 - b_2} J_0, \quad (20)$$

and

$$\varepsilon_{2\mathbf{k}} = (b_1 - b_2)J_0 + D(ak)^2 \quad (21)$$

for in-phase and antiphase precession of sublattice magnetization, respectively. Here we used the quadratic expansion when evaluating the quantity  $J_0 - J_{\mathbf{k}} \approx zJ(ak)^2 = J_0(ak)^2$  (here  $z$  is the number of nearest neighbors, and  $a$  stands for the lattice spacing).

As already mentioned, the poles of  $\chi^{zz}(\mathbf{q}, \omega)$  define the energy of longitudinal excitations in the system. Due to rather complex dependence of the function on frequency, we shall consider real and imaginary parts of  $D(\mathbf{q}, \omega)$  only in some limiting cases. Namely, we investigate this function near the singularities of  $\Phi(q)$ ,  $\Pi(q)$ , and  $B(q)$ . That is when one of the equations  $\omega(\mathbf{q}) = \varepsilon_{1\mathbf{p}} - \varepsilon_{1\mathbf{p}-\mathbf{q}}$ , or  $\omega(\mathbf{q}) = \varepsilon_{2\mathbf{p}} - \varepsilon_{2\mathbf{p}-\mathbf{q}}$ , or  $\omega(\mathbf{q}) = \varepsilon_{1\mathbf{p}} + \varepsilon_{2\mathbf{p}-\mathbf{q}}$  is fulfilled, i.e., when the related virtual two-spin-wave creation/annihilation processes are most effective. For reasons which will be explained below, we will call the branch of longitudinal excitations due to creation and annihilation of the same (both acoustic or both exchange) spin waves the ‘‘acoustic’’ longitudinal spin excitations; we will call the branch of longitudinal excitations due to creation and annihilation of different (one acoustic and one exchange) transverse spin waves the ‘‘exchange’’ longitudinal spin excitations.

### A. Acoustic longitudinal spin excitations

Let us start with the singularity in  $\chi^{zz}(\mathbf{q}, \omega)$  due to virtual processes of creation and annihilation of two spin waves with in-phase or antiphase sublattice magnetization precession (the first and second channels of longitudinal excitations). Quantitative analysis given in Appendix C shows that these processes will provide the main contribution in the denominator  $D(\mathbf{q}, \omega)$  if the parameter

$$a^\pm = \frac{q}{2} \pm \frac{\omega}{2Dq} \quad (22)$$

is small enough, i.e.,  $|a^\pm| \ll 1$ . (Hereinafter we suppose that the conventional analytic continuation is made, i.e.,  $i\omega_n \rightarrow \omega + i\delta$ .) In this approximation, i.e., ignoring the third channel, after simple algebra, the real and imaginary parts of expression (18) can be written as

$$\begin{aligned} \text{Re } D(\mathbf{q}, \omega) &\approx 1 - J_{\mathbf{q}} \frac{b_1^2 b_2^2}{(b_1 - b_2)^2} \{2 \text{Re}(\lambda_1^+ + \lambda_1^- - \lambda_2^+ - \lambda_2^-) \\ &\quad - J_{\mathbf{q}}(b_1 + b_2)^2 [\text{Re}(\lambda_1^+ + \lambda_1^-) \text{Re}(\lambda_2^+ + \lambda_2^-) \\ &\quad - \text{Im}(\lambda_1^+ + \lambda_1^-) \text{Im}(\lambda_2^+ + \lambda_2^-)]\}, \quad (23) \\ \text{Im } D(\mathbf{q}, \omega) &\approx -J_{\mathbf{q}} \frac{b_1^2 b_2^2}{(b_1 - b_2)^2} \{2 \text{Im}(\lambda_1^+ + \lambda_1^- - \lambda_2^+ - \lambda_2^-) \\ &\quad - J_{\mathbf{q}}(b_1 + b_2)^2 [\text{Re}(\lambda_1^+ + \lambda_1^-) \text{Im}(\lambda_2^+ + \lambda_2^-) \\ &\quad + \text{Im}(\lambda_1^+ + \lambda_1^-) \text{Re}(\lambda_2^+ + \lambda_2^-)]\}. \quad (24) \end{aligned}$$

The explicit form of the real and imaginary parts of additional functions  $\lambda_i^\pm = \lambda_i^\pm(\mathbf{q}, \omega)$  [(C1)–(C3)] introduced here are presented in Appendix C. After simple but cumbersome calculations (some details can be found in Appendix C), we obtain for the leading part of the longitudinal spin susceptibility

$$\chi^{zz}(\mathbf{q}, \omega) \sim i \frac{(b_1 - b_2)^4}{b_1^2 b_2^2} \left( \frac{J_0}{J_{\mathbf{q}}} \right)^2 \frac{N(\mathbf{q}, \omega)}{(\omega^2 - \Omega_{\text{res}}^2)(\omega^2 - \Omega_{\text{dif}}^2)}, \quad (25)$$

where the characteristic frequencies are

$$\begin{aligned} \Omega_{\text{res(dif)}}^2 / (Dq)^2 &= 6 + iA(T) \\ &\pm \left\{ [6 + iA(T)]^2 - 3\pi \frac{(b_1 - b_2)^2}{b_1 b_2} [\pi \right. \\ &\quad \left. - i6(b_1 + b_2)] \arctg \left( \frac{2b_1 b_2}{(b_1 - b_2)^2} \right) \right\}^{1/2}, \quad (26) \end{aligned}$$

where

$$A(T) = \pi(b_1 + b_2) \left[ 1 + 3 \frac{(b_1 - b_2)^2}{4b_1 b_2} \arctg \left( \frac{2b_1 b_2}{(b_1 - b_2)^2} \right) \right].$$

In particular, in a temperature region near the Curie one, when  $b_1 \approx b_2$  and is small, the expressions for longitudinal vibrations acquire a simple form,

$$\begin{aligned} \Omega_{\text{res}} &\approx 3.46Dq + i\gamma(q, T), \quad (27) \\ \gamma(q, T) &\sim \frac{3}{2} \pi^2 \frac{(b_1 + b_2)^2}{b_1 b_2} Dq. \end{aligned}$$

For the diffusive mode, one obtains

$$\Omega_{\text{dif}} \approx 0.8\pi \frac{(b_1 - b_2)}{\sqrt{b_1 b_2}} Dq \{a(T) - ic(T)\}^{1/2}, \quad (28)$$

where

$$\begin{aligned} a(T) &= 6\pi \frac{1 - (b_1 + b_2)^2}{36 + \pi^2(b_1 + b_2)^2}, \\ c(T) &= (b_1 + b_2) \frac{36 + \pi^2}{36 + \pi^2(b_1 + b_2)^2}. \end{aligned}$$

Thus, in the  $(\mathbf{q}, \omega)$  region where the condition  $|a^\pm| \ll 1$  is fulfilled, the function  $\chi^{zz}(\mathbf{q}, \omega)$  possesses two types of resonances. There is a peak which characterizes a precessionlike motion with the frequency  $\pm\Omega_{\text{res}} \sim Dq$  and damping  $\gamma(q) \sim Dq$ ; both these functions linearly depend on the wave vector (the acoustic branch longitudinal spin excitations). This allows us to affirm that in the system the wavelike vibrations of spin longitudinal components exist, although with strong attenuation. At the same time, there is also a quasidiffusive pole at  $\pm i\Omega_{\text{dif}}$ , i.e., the quasirelaxation mode connected to diffusion of longitudinal fluctuations, which forms the central peak in the spectral function  $\frac{1}{\omega} \text{Im } \chi^{zz}(\mathbf{q}, \omega)$ . Thus, in the frequency and wave vector region under consideration, Eq. (22), the ferrimagnet spectral function behavior is similar to those in the case of a ferromagnet [21].

The susceptibility and the longitudinal spin fluctuations at temperature close to  $T_C$  can be directly determined by inelastic scattering of polarized neutrons. In these experiments, a spin polarization analysis of the data gives the possibility to distinguish contributions from longitudinal and transverse spin modes (for more details see, e.g., [29] and references therein).

Note here, to avoid confusion, that applicability the results obtained in the  $(\mathbf{q}, \omega)$  area for the frequency is determined by the conditions  $\omega(\mathbf{q}) \approx \varepsilon_{1\mathbf{p}} - \varepsilon_{1\mathbf{p}-\mathbf{q}}$  and  $\omega(\mathbf{q}) \approx \varepsilon_{2\mathbf{p}} - \varepsilon_{2\mathbf{p}-\mathbf{q}}$ , while a restriction on the wave vector is conditioned by proximity to the hydrodynamic regime, where the physics of the magnetization dynamics is determined by the magnetization conservation laws [30]. As is already known, the RPA

results remain valid beyond the hydrodynamic regime, i.e., when the wave vector is larger than the inverse correlation length  $\xi$ :  $q > 1/\xi \sim (1 - T/T_C)^{1/2}$ , and, of course, beyond the critical region (for more details see, e.g., Refs. [21,25]). (A second-order phase transition takes place in the system at a temperature  $T_C = 1/3[S_1 S_2 (S_1 + 1)(S_2 + 1)]^{1/2} J_0$  [20].)

### B. Exchange longitudinal spin excitations

We are now in a position to consider a central result of the paper, that is, longitudinal excitations due to virtual creation and annihilation transverse spin waves of different branches (the third channel of longitudinal excitations). Quantitative analysis (see Appendix C for details) indicates that these virtual processes will cause a singularity in  $\chi^{zz}(\mathbf{q}, \omega)$  if the parameter

$$b^\pm = \frac{q}{2} + \left[ \frac{q^2}{4} + \frac{(b_1 - b_2)J_0 \pm \omega}{2D} \right]^{1/2} \quad (29)$$

is small enough, i.e.,  $|b^\pm| \ll 1$ . In this approximation, after simple algebra, the leading part of the denominator (18) that determines the dispersion law and damping of longitudinal spin excitations can be written as

$$D(\mathbf{q}, \omega_q) \approx 1 - 2J_q \Phi(\mathbf{q}, \omega_q). \quad (30)$$

$$\gamma(q, \Omega_{\text{exc}}) \sim 2\pi b_1 b_2 \frac{J_0^2}{T} \left\{ 1 - \kappa_0^2 + \frac{T}{D} \ln \left[ \frac{(b_1 - b_2)J_0 + D}{(b_1 - b_2)J_0 + D\kappa_0^2} \right] + \frac{T}{D} \ln \left( \kappa_0^2 \left[ \frac{4b_1 b_2}{(b_1 - b_2)^2} \right]^2 \right) \right\}, \quad (34)$$

where

$$\kappa_0^2 = \frac{(b_1 - b_2)^2}{4b_1 b_2} \left[ 2 \ln \frac{T}{(b_1 - b_2)J_0} + \frac{\pi^2}{2} + f(T)q \right]. \quad (35)$$

Thus, the ratio  $\gamma(q, \Omega_{\text{exc}})/\Omega_{\text{exc}}(q, T)$  is approximately  $\gamma(q, \Omega_{\text{exc}})/\Omega_{\text{exc}}(q, T) \sim \frac{b_1 b_2 J_0}{b_1 - b_2 T}$ , and at low temperature  $T < J_0$  it is large enough. But at  $T \sim T_C$   $b_1 \ll S_1$ ,  $b_2 \ll S_2$ , and  $\gamma(q, \Omega_{\text{exc}})/\Omega_{\text{exc}}(q, T) \sim \frac{(b_1/S_1)(b_2/S_2)}{b_1 - b_2} \ll 1$  is smaller than unity. This allows us to affirm that in a ferrimagnet wavelike excitations of longitudinal components of magnetization exist, although with strong attenuation at low temperature.

As follows from direct examination of the functions  $Q(q)$  [Eq. (B3)] and  $\Lambda(q)$  [Eq. (B4)], the physical mechanism of the spin longitudinal excitations remains valid in the high approximation, too. We investigated these functions in the frequency  $\omega$  and momentum  $\mathbf{q}$  domains where parameters (22) and (29) are small enough and found that the account of the two-loop diagrams has not caused principal corrections to the energy and damping of longitudinal spin excitations. (The related analysis will be published elsewhere.)

## V. DISCUSSION

It is now commonly accepted that the ultrafast magnetization process proceeds with several important characteristic time scales [1,31–33]: (i) a femtosecond demagnetization, (ii) a picosecond recovery, and (iii) a nanosecond magneti-

Calculations show that now the leading part of the longitudinal spin susceptibility reads

$$\chi^{zz}(\mathbf{q}, \omega) \sim \frac{(b_1 - b_2)^4 J_0}{2b_1^2 b_2^2} \frac{N(\mathbf{q}, \omega)}{J_q \pm \omega + \Omega_{\text{exc}} + i\gamma_{\text{exc}}}. \quad (31)$$

The quantity  $\Omega_{\text{exc}} = \Omega_{\text{exc}}(q, T)$  should be considered the frequencies of collective vibrations of magnetization longitudinal components, which in this  $(\mathbf{q}, \omega)$  region are described by the following expression (see Appendix C):

$$\Omega_{\text{exc}}(q, T) \approx (b_1 - b_2)J_0 \left[ 1 + 2 \ln \frac{T}{(b_1 - b_2)J_0} + \frac{\pi^2}{2} + f(T)q \right], \quad (32)$$

where

$$f(T) \approx 4 \frac{J_0^2}{T J_q} + \ln \left[ \frac{(b_1 + b_2)J_0 + D}{T} Dq \right] - 2 \left( 1 + \frac{3D}{4T} \right). \quad (33)$$

By analogy to the terminology for the transverse spin wave oscillations, we will call this type of longitudinal excitation the exchange longitudinal spin excitations. Note that the exchange longitudinal mode is energetically above the exchange mode of the transverse spin wave (21) at the same temperature and wave vector, and liner depends on  $q$ .

For the damping of the exchange longitudinal mode, we obtained

zation precession and relaxation, traditionally characterized by the ferromagnetic resonance frequency and the Landau-Lifshitz-Gilbert (LLG) damping parameter. It is also generally recognized that the physics of magnetization changes on femtosecond time scales requires understanding the role of different subsystems (photons, phonons, electrons) in the angular momentum transfer [1,31,32], too. Concerning multisublattice magnetic materials, an additional question arises about the effect which the magnetization or angular momentum compensation point plays in ultrafast longitudinal magnetization dynamics (see, e.g., [7,8] and references therein).

The first attempts to describe longitudinal magnetization dynamics in two-sublattice systems have been proposed recently [13,14,16,17]. Based on the existing experimental results and from a general point of view, it was suggested that the longitudinal relaxation and the transverse relaxation (the LLG damping) are independent quantities. That is, as in the case of nanoscale magnetism (see reviews [34,35] and references therein), there is a longitudinal relaxation time which fits a direct path to the thermal bath and a so-called transverse time which represents scattering into the transverse magnetization components. The main feature of the phenomenological dynamic equations proposed that made them suitable for the ultrafast magnetization dynamics is the presence of a longitudinal relaxation term coming from the strong exchange interaction between spins. Since the exchange fields are large (10–100 T), the corresponding

characteristic longitudinal relaxation time scale is of the order of 10–100 fs and thus manifests itself in the ultrafast processes.

On the other hand, it is obvious that for exhaustive understanding of the underlying physics of ultrafast magnetization dynamics a microscopic description of longitudinal magnetization dynamics in the equilibrium state of the system is strongly required. Distinctive features of the longitudinal dynamics in the multisublattice magnet equilibrium state have to be a datum point in attempts to understand the dynamics of a ferrimagnet after femtosecond laser pulse heating far beyond an equilibrium state. Keeping in mind that the Heisenberg model deals exclusively with spin degrees of freedom, let us make some estimation concerning the suggestions made in the phenomenological models with the same approximation.

In the models in Refs. [16,17] the authors suggest that the dynamics of the length of the sublattice magnetizations is pertinent to the time scale of the exchange interaction and that on this time scale the conventional transverse dynamics of the angular momentum is negligible. Particularly, in this approximation longitudinal exchange relaxation in magnets with only one sublattice is not possible. However, following our consideration, in two-sublattice magnets there are additional equal-in-value channels of the longitudinal mode relaxation by which energy is scattered into the transverse magnetization component. Note also that according to Izyumov *et al.* [21], in one-sublattice magnets a longitudinal spin mode relaxes due to a virtual process of creation and annihilation of ordinary spin waves, too.

In Ref. [11] the authors, using conventional suggestions about the spin wave spectrum in a ferrimagnetic system, discuss the role which the magnetization or angular momentum compensation point plays in thermally induced magnetization switching. The authors consider the classical spin Heisenberg model, and thus, the thermal equilibrium distribution of the spin fluctuations rests on the classical limit (see the Supplementary Information in [11]). Based on these suggestions, the authors conclude that the switching is caused by the excitation of two-magnon bound states.

However, the microscopic calculation using the diagram technique for spin operators [36] shows that near the angular momentum compensation point  $T_L$  the system behavior is not the classical one. In particular, the energy of the in-phase precession of the magnetizations of the sublattices becomes higher than that of the out-of-phase precession; near  $T_L$  fluctuations in the weak sublattice magnetization have a significant influence on the resonance properties of the system, with different temperature behaviors of the in-phase and out-of-phase precessions of the sublattice magnetization. Also, the occupation numbers for the acoustic magnons become large, and a finite number of spin operator states  $(2S + 1)$  takes on special significance. In other words, the difference in quantum nature of Bose and spin operators is fundamental for understanding the magnetization dynamics in the neighborhood of the compensation points, too.

Based on our results, thermally induced magnetization switching most likely comes from emission/absorption of two transverse spin waves which are not in bound states. However, we stress that in this paper we consider a ferrimagnet without a compensation point. A ferrimagnetic system with compensation points requires special consideration, in particular because

at high enough temperature a weak sublattice dynamics is, in fact, a paramagnetic precession of magnetization in the exchange field of a strong sublattice (for more details see [36] and reference therein). Note in this connection that the case of a compensated antiferromagnet ( $S_1 = S_2$ ,  $g_1 = g_2$ ) also calls for a special analysis in view of the strong dependence of its properties on the anisotropic interactions.

In conclusion, in this paper, in the framework of a quantum-mechanical approach, the general expression for longitudinal spin susceptibility  $\chi^{zz}(\mathbf{q}, \omega)$  of a two-sublattice Heisenberg ferrimagnet was obtained with the aim to overcome limitations typical of the phenomenological approaches. Our microscopic analysis utilizes the diagram techniques for the spin operators, which formally yield analytic expressions that are valid over the entire temperature range of the magnetically ordered state of the system. Namely, the results are applicable in the  $(\mathbf{q}, \omega)$  space beyond both hydrodynamical and critical regimes.

Strong renormalization of the magnetization longitudinal vibration due to a few channels of virtual creation and annihilation of transverse spin waves has been found. Videlicet, there is a process of creation and annihilation of two spin (acoustic) waves at frequencies  $\omega(\mathbf{q}) = (\varepsilon_{1\mathbf{k}} - \varepsilon_{1\mathbf{k}\pm\mathbf{q}})$  which corresponds to in-phase sublattice magnetization precession and is in close analogy to a ferromagnet case. There is also a channel of two spin wave excitations with the energies  $\varepsilon_{2\mathbf{k}}$  and  $\varepsilon_{2\mathbf{k}\pm\mathbf{q}}$ , which correspond to out-of-phase sublattice magnetization precession (exchange spin waves). The third channel is a two-spin-wave creation/annihilation process at frequency  $\omega(\mathbf{q}) = (\varepsilon_{1\mathbf{k}} + \varepsilon_{2\mathbf{k}\pm\mathbf{q}})$ . (In all these processes the wave vector  $\mathbf{k}$  is a variable.) The first two channels are controlled by the occupation factor determined through the spin wave Bose distribution function. However, the processes of creation or annihilation of one acoustic and one exchange mode (the third channel) remain effective even in the absence of transverse excitations, i.e., when  $n(\varepsilon_{\mathbf{k}}) \rightarrow 0$ , and, in our opinion, most likely provide the main contribution to the thermally induced magnetization reversal.

We have shown that the spectrum of longitudinal excitations consists of a quasirelaxation mode forming a central peak in  $\chi^{zz}(\mathbf{q}, \omega)$  and two (acoustic and exchange) precessionlike modes. As the main result, it is predicted that both acoustic and exchange longitudinal excitations are energetically above similar modes of transverse spin waves at the same temperature and wave vector. The existence of such a high-energy exchange longitudinal mode reveals the possibility for a new form of excitation behavior in ferrimagnetic materials. Also, our analysis indicates that in a temperature region near the Curie one the main contribution to the longitudinal magnetization relaxation comes from the high-frequency spin waves. This process occurs due to a strong exchange field. As a result, the longitudinal relaxation time (the inverse longitudinal relaxation rate) is much faster than transverse spin wave damping.

The existing experimental results indicate that in a ferrimagnetic system the ultrafast magnetization reversal occurs due to intrinsic material properties, but so far the microscopic mechanism responsible for the reversal has not been identified. We hope that the results obtained in this paper within a consistent microscopic theory will be important for understanding the physics of nonequilibrium magnetic dynamics under the effect of ultrafast laser pulses in multisublattice magnetic materials.

## ACKNOWLEDGMENTS

The author is grateful for valuable discussions with V. G. Bar'yakhtar and B. A. Ivanov. This work is partly supported by the European Union Horizon 2020 Research and Innovation Programme under Marie Skłodowska-Curie Grant Agreement No. 644348 (MagIC).

## APPENDIX A: TRANSVERSE GFS IN THE HARTREE-FOCK APPROXIMATION

To calculate the transverse GFs,  $G_{ij}(q) = -1/2\langle\langle\widehat{T}S_{ig}^+|S_{jf}^-\rangle\rangle|_{q,\omega}$  ( $i, j = 1, 2$ ), we use the Larkin equation derived earlier in the framework of the diagrammatic technique for spin operators (see, for instance, [22,23]). In that case, each connected diagram for the transverse GFs can be represented in the form of single-cell blocks  $\Sigma_{ij}(q)$  joined by the interaction lines  $J_q$  (the Fourier transform of the exchange interaction). It can be shown that the total (infinite) graph series for transverse GFs of a two-sublattice ferrimagnet obeys the system of equations

$$\begin{aligned} G_{ii}(q) &= \Sigma_{ii}(q) + \Sigma_{ii}(q)J_q G_{ji}(q), \\ G_{ji}(q) &= \Sigma_{ji}(q) + \Sigma_{jj}(q)J_q G_{ii}(q). \end{aligned}$$

In terms of the diagrammatic technique, the quantity  $\Sigma_{ij}(q)$  should be called the part uncuttable across a line of interaction  $J_q$ . All ‘‘cuttable’’ parts are compressed into the second term on the right-hand sides of these equations. Dealing with transverse spin wave excitations, we are interested in summation of graphical series for the GFs in the Hartree-Fock approximation. In this approximation, a graphical representation of the systems of equations for the transverse  $G_{11}(q)$  and  $G_{12}(q)$  and also  $G_{22}(q)$  and  $G_{21}(q)$  GFs are shown in Figs. 2(a) and 2(b), respectively. Here thick (thin) lines represent dressed [undressed,  $K_{ii}(q)$ ] GFs; the wavy line corresponds to the interaction  $J_q$ . The open points indicate vertices corresponding to the operators  $S_i^z$  ( $i = 1, 2$ ). These equations in the Fourier transformed form read

$$G_{11}(q) = b_1 K_{11}(i\omega_n) + b_1 K_{11}(i\omega_n)J_q G_{21}(q), \quad (\text{A1})$$

$$G_{21}(q) = -b_2 K_{22}(i\omega_n)J_q G_{11}(q). \quad (\text{A2})$$

The system of equations for the next pair of coupled functions,  $G_{22}(q)$  and  $G_{12}(q)$ , possesses a very similar structure. Here

$K_{11}(i\omega_n) = 1/(i\omega_n + y_0)$  and  $K_{22}(i\omega_n) = 1/(i\omega_n - x_0)$  are (undressed) GFs in the mean-field approximation. We used the notations  $b_1 \equiv b_1(\beta y S_1) = \langle S_1^z \rangle^{(0)}$  and  $b_2 \equiv b_2(\beta x S_2) = \langle S_2^z \rangle^{(0)}$ , which are the magnetization of the first and second sublattices, respectively.

Using these equations, for the GFs describing transverse spin precessions we obtained

$$G_{11}(q) = \frac{b_1 K_{22}^{-1}(i\omega_n)}{(i\omega_n + \varepsilon_{1q})(i\omega_n - \varepsilon_{2q})}, \quad (\text{A3})$$

$$G_{12}(q) = G_{21}(q) = -\frac{b_1 b_2 J_q}{(i\omega_n + \varepsilon_{1q})(i\omega_n - \varepsilon_{2q})}, \quad (\text{A4})$$

$$G_{22}(q) = -\frac{b_2 K_{11}^{-1}(i\omega_n)}{(i\omega_n + \varepsilon_{1q})(i\omega_n - \varepsilon_{2q})}. \quad (\text{A5})$$

Here and below, for shorthand notation, we introduce the designation  $\varepsilon_i(\mathbf{q}) = \varepsilon_{i\mathbf{q}}$ . These GFs describe the propagation of spin waves with the momentum  $\mathbf{q}$  and energy

$$\begin{aligned} \varepsilon_{1q} &= -\frac{1}{2}(b_1 - b_2)J_0 + \frac{1}{2}[(b_1 - b_2)^2 J_0^2 \\ &\quad + 4b_1 b_2 (J_0^2 - J_q^2)]^{1/2} \end{aligned} \quad (\text{A6})$$

for an acoustic spin wave with an in-phase precession of the sublattice magnetization and energy

$$\begin{aligned} \varepsilon_{2q} &= \frac{1}{2}(b_1 - b_2)J_0 + \frac{1}{2}[(b_1 - b_2)^2 J_0^2 \\ &\quad + 4b_1 b_2 (J_0^2 - J_q^2)]^{1/2} \end{aligned} \quad (\text{A7})$$

for an exchange spin wave with an antiphase precession of the sublattice magnetization. In a long-wave limit ( $aq \ll 1$ ), the asymptotic expansions provide expressions (20) and (21), respectively.

## APPENDIX B: ANALYTICAL EXPRESSIONS FOR THE LOOP DIAGRAMS

To calculate the loop diagrams  $\Phi(q)$ ,  $\Pi(q)$ ,  $B(q)$ ,  $Q(q)$ , and  $\Lambda(q)$ , where  $q = \{\mathbf{q}, i\omega_n\}$ , we substitute the spin wave GFs (A3)–(A5) into Eqs. (10)–(14) and sum up over the discrete Matsubara frequencies. Simple but cumbersome calculations give, for the function  $\Phi(q)$ , analytical expression (19). For functions  $\Pi(q)$ ,  $B(q)$ ,  $Q(q)$ , and  $\Lambda(q)$  similar calculations yield

$$\begin{aligned} \Pi(q) &= \frac{b_1^2}{N} \sum_{\mathbf{p}} \left\{ \frac{\varepsilon_{1\mathbf{p}} - x}{\varepsilon_{1\mathbf{p}} + \varepsilon_{2\mathbf{p}}} \frac{\varepsilon_{1\mathbf{p}-\mathbf{q}} - x}{\varepsilon_{1\mathbf{p}-\mathbf{q}} + \varepsilon_{2\mathbf{p}-\mathbf{q}}} \frac{n_1(\varepsilon_{1\mathbf{p}}) - n_1(\varepsilon_{1\mathbf{p}-\mathbf{q}})}{i\omega_q - \varepsilon_{1\mathbf{p}} + \varepsilon_{1\mathbf{p}-\mathbf{q}}} - \frac{\varepsilon_{2\mathbf{p}} + x}{\varepsilon_{1\mathbf{p}} + \varepsilon_{2\mathbf{p}}} \frac{\varepsilon_{1\mathbf{p}-\mathbf{q}} - x}{\varepsilon_{1\mathbf{p}-\mathbf{q}} + \varepsilon_{2\mathbf{p}-\mathbf{q}}} \frac{1 + n_1(\varepsilon_{1\mathbf{p}-\mathbf{q}}) + n_2(\varepsilon_{2\mathbf{p}})}{i\omega_q + \varepsilon_{2\mathbf{p}} + \varepsilon_{1\mathbf{p}-\mathbf{q}}} \right. \\ &\quad \left. + \frac{\varepsilon_{1\mathbf{p}} - x}{\varepsilon_{1\mathbf{p}} + \varepsilon_{2\mathbf{p}}} \frac{\varepsilon_{1\mathbf{p}-\mathbf{q}} + x}{\varepsilon_{1\mathbf{p}-\mathbf{q}} + \varepsilon_{2\mathbf{p}-\mathbf{q}}} \frac{1 + n_1(\varepsilon_{1\mathbf{p}}) + n_2(\varepsilon_{2\mathbf{p}-\mathbf{q}})}{i\omega_q - \varepsilon_{1\mathbf{p}} - \varepsilon_{2\mathbf{p}-\mathbf{q}}} + \frac{\varepsilon_{2\mathbf{p}} + x}{\varepsilon_{1\mathbf{p}} + \varepsilon_{2\mathbf{p}}} \frac{\varepsilon_{2\mathbf{p}-\mathbf{q}} + x}{\varepsilon_{1\mathbf{p}-\mathbf{q}} + \varepsilon_{2\mathbf{p}-\mathbf{q}}} \frac{n_2(\varepsilon_{2\mathbf{p}-\mathbf{q}}) - n_2(\varepsilon_{2\mathbf{p}})}{i\omega_q + \varepsilon_{2\mathbf{p}} - \varepsilon_{2\mathbf{p}-\mathbf{q}}} \right\}, \quad (\text{B1}) \end{aligned}$$

$$\begin{aligned} B(q) &= \frac{b_2^2}{N} \sum_{\mathbf{p}} \left\{ \frac{\varepsilon_{2\mathbf{p}} - y}{\varepsilon_{1\mathbf{p}} + \varepsilon_{2\mathbf{p}}} \frac{\varepsilon_{2\mathbf{p}-\mathbf{q}} - y}{\varepsilon_{1\mathbf{p}-\mathbf{q}} + \varepsilon_{2\mathbf{p}-\mathbf{q}}} \frac{n_2(\varepsilon_{2\mathbf{p}-\mathbf{q}}) - n_2(\varepsilon_{2\mathbf{p}})}{i\omega_q - \varepsilon_{2\mathbf{p}} + \varepsilon_{2\mathbf{p}-\mathbf{q}}} - \frac{\varepsilon_{1\mathbf{p}} + y}{\varepsilon_{1\mathbf{p}} + \varepsilon_{2\mathbf{p}}} \frac{\varepsilon_{2\mathbf{p}-\mathbf{q}} - y}{\varepsilon_{1\mathbf{p}-\mathbf{q}} + \varepsilon_{2\mathbf{p}-\mathbf{q}}} \frac{1 + n_1(\varepsilon_{1\mathbf{p}}) + n_2(\varepsilon_{2\mathbf{p}-\mathbf{q}})}{i\omega_q - \varepsilon_{1\mathbf{p}} - \varepsilon_{2\mathbf{p}-\mathbf{q}}} \right. \\ &\quad \left. - \frac{\varepsilon_{2\mathbf{p}} - y}{\varepsilon_{1\mathbf{p}} + \varepsilon_{2\mathbf{p}}} \frac{\varepsilon_{2\mathbf{p}} - y}{\varepsilon_{1\mathbf{p}-\mathbf{q}} + \varepsilon_{2\mathbf{p}-\mathbf{q}}} \frac{1 + n_1(\varepsilon_{1\mathbf{p}-\mathbf{q}}) + n_2(\varepsilon_{2\mathbf{p}})}{i\omega_q + \varepsilon_{2\mathbf{p}} + \varepsilon_{1\mathbf{p}-\mathbf{q}}} + \frac{\varepsilon_{1\mathbf{p}} + y}{\varepsilon_{1\mathbf{p}} + \varepsilon_{2\mathbf{p}}} \frac{\varepsilon_{1\mathbf{p}-\mathbf{q}} + y}{\varepsilon_{1\mathbf{p}-\mathbf{q}} + \varepsilon_{2\mathbf{p}-\mathbf{q}}} \frac{n_1(\varepsilon_{1\mathbf{p}}) - n_1(\varepsilon_{1\mathbf{p}-\mathbf{q}})}{i\omega_q + \varepsilon_{1\mathbf{p}} - \varepsilon_{1\mathbf{p}-\mathbf{q}}} \right\}, \quad (\text{B2}) \end{aligned}$$

$$Q(q) = \frac{b_1^2 b_2}{N} \sum_{\mathbf{p}} \frac{J_{\mathbf{p}}^2}{\varepsilon_{1\mathbf{p}} + \varepsilon_{2\mathbf{p}}} \left\{ \frac{\varepsilon_{1\mathbf{p}-\mathbf{q}} - x}{\varepsilon_{1\mathbf{p}-\mathbf{q}} + \varepsilon_{2\mathbf{p}-\mathbf{q}}} \left( \frac{n_1(\varepsilon_{1\mathbf{p}}) - n_1(\varepsilon_{1\mathbf{p}-\mathbf{q}})}{i\omega_q - \varepsilon_{1\mathbf{p}} + \varepsilon_{1\mathbf{p}-\mathbf{q}}} + \frac{1 + n_1(\varepsilon_{1\mathbf{p}-\mathbf{q}}) + n_2(\varepsilon_{2\mathbf{p}})}{i\omega_q + \varepsilon_{2\mathbf{p}} + \varepsilon_{1\mathbf{p}-\mathbf{q}}} \right) \right. \\ \left. + \frac{\varepsilon_{1\mathbf{p}-\mathbf{q}} + x}{\varepsilon_{1\mathbf{p}-\mathbf{q}} + \varepsilon_{2\mathbf{p}-\mathbf{q}}} \left( \frac{1 + n_1(\varepsilon_{1\mathbf{p}}) + n_2(\varepsilon_{2\mathbf{p}-\mathbf{q}})}{i\omega_q - \varepsilon_{1\mathbf{p}} - \varepsilon_{2\mathbf{p}-\mathbf{q}}} + \frac{n_2(\varepsilon_{2\mathbf{p}}) - n_2(\varepsilon_{2\mathbf{p}-\mathbf{q}})}{i\omega_q + \varepsilon_{2\mathbf{p}} - \varepsilon_{2\mathbf{p}-\mathbf{q}}} \right) \right\}, \quad (\text{B3})$$

$$\Lambda(q) = \frac{b_1 b_2^2}{N} \sum_{\mathbf{p}} \frac{J_{\mathbf{p}}^2}{\varepsilon_{1\mathbf{p}} + \varepsilon_{2\mathbf{p}}} \left\{ \frac{\varepsilon_{2\mathbf{p}-\mathbf{q}} - y}{\varepsilon_{1\mathbf{p}-\mathbf{q}} + \varepsilon_{2\mathbf{p}-\mathbf{q}}} \left( \frac{1 + n_1(\varepsilon_{1\mathbf{p}}) + n_2(\varepsilon_{2\mathbf{p}-\mathbf{q}})}{i\omega_q - \varepsilon_{1\mathbf{p}} - \varepsilon_{2\mathbf{p}-\mathbf{q}}} - \frac{n_2(\varepsilon_{2\mathbf{p}-\mathbf{q}}) - n_2(\varepsilon_{2\mathbf{p}})}{i\omega_q - \varepsilon_{2\mathbf{p}-\mathbf{q}} + \varepsilon_{2\mathbf{p}}} \right) \right. \\ \left. + \frac{\varepsilon_{1\mathbf{p}-\mathbf{q}} + y}{\varepsilon_{1\mathbf{p}-\mathbf{q}} + \varepsilon_{2\mathbf{p}-\mathbf{q}}} \left( \frac{1 + n_1(\varepsilon_{1\mathbf{p}-\mathbf{q}}) + n_2(\varepsilon_{2\mathbf{p}})}{i\omega_q + \varepsilon_{1\mathbf{p}-\mathbf{q}} + \varepsilon_{2\mathbf{p}}} + \frac{n_1(\varepsilon_{1\mathbf{p}}) - n_1(\varepsilon_{1\mathbf{p}-\mathbf{q}})}{i\omega_q - \varepsilon_{1\mathbf{p}} + \varepsilon_{1\mathbf{p}-\mathbf{q}}} \right) \right\}. \quad (\text{B4})$$

Here  $n_1(\varepsilon_{1\mathbf{p}})$  and  $n_2(\varepsilon_{2\mathbf{p}})$  are the Bose distribution functions for excitations with in-phase and out-of-phase sublattice oscillations, respectively (i.e., acoustic and exchange spin waves).

### APPENDIX C: CALCULATION OF THE LOOP DIAGRAMS

To find the asymptotic of loop diagrams  $\Phi(q)$ ,  $\Pi(q)$ ,  $B(q)$ ,  $Q(q)$ , and  $\Lambda(q)$  we will use the approximation  $\varepsilon_{1\mathbf{p}} + \varepsilon_{2\mathbf{p}} \approx (b_1 - b_2)J_0$ ,  $\varepsilon_{1\mathbf{p}} - x \approx -b_2J_0$ ,  $\varepsilon_{2\mathbf{p}} + x \approx b_1J_0$ ,  $\varepsilon_{2\mathbf{p}} - y \approx -b_2J_0$ , and  $\varepsilon_{1\mathbf{p}} + y \approx b_2J_0$  in Eqs. (19) and (B1)–(B4) for the factors at the singularities. Then the quantities on the left-hand sides of Eqs. (19) and (B1)–(B4) can be expressed in terms of the universal functions defined as

$$\lambda_i(\mathbf{q}, \omega) = \frac{1}{N} \sum_{\mathbf{p}} \frac{n_i(\varepsilon_{i\mathbf{p}})}{\omega - \varepsilon_{i\mathbf{p}} + \varepsilon_{i\mathbf{p}-\mathbf{q}} + i\delta}, \quad (\text{C1})$$

$$\lambda_0(\mathbf{q}, \omega) = \frac{1}{N} \sum_{\mathbf{p}} \frac{1}{\omega - \varepsilon_{1\mathbf{p}} - \varepsilon_{2\mathbf{p}-\mathbf{q}} + i\delta}, \quad (\text{C2})$$

$$\lambda_{0i}(\mathbf{q}, \omega) = \frac{1}{N} \sum_{\mathbf{p}} \frac{n_i(\varepsilon_{i\mathbf{p}})}{\omega - \varepsilon_{i\mathbf{p}} + \varepsilon_{j\mathbf{p}-\mathbf{q}} + i\delta}, \quad i \neq j, \quad (\text{C3})$$

where  $i, j = 1, 2$ . Namely, after simple algebra we can write  $\Phi(q)$ ,  $Q(q)$ , and  $B(q)$  in the form

$$\Phi(q) = \frac{b_1^2 b_2^2}{(b_1 - b_2)^2} (\lambda_1^+ + \lambda_1^- - \lambda_2^+ - \lambda_2^- - \lambda_0^+ - \lambda_0^- - \lambda_{01}^+ - \lambda_{01}^- - \lambda_{02}^+ - \lambda_{02}^-),$$

$$\Pi(q) = \frac{b_1^2}{(b_1 - b_2)^2} \{b_2^2(\lambda_1^+ + \lambda_1^-) - b_1^2(\lambda_2^+ + \lambda_2^-) - b_1 b_2(\lambda_0^+ + \lambda_0^- + \lambda_{01}^+ + \lambda_{01}^- + \lambda_{02}^+ + \lambda_{02}^-)\},$$

$$B(q) = \frac{b_2^2}{(b_1 - b_2)^2} \{b_1^2(\lambda_1^+ + \lambda_1^-) - b_2^2(\lambda_2^+ + \lambda_2^-) - b_1 b_2(\lambda_0^+ + \lambda_0^- + \lambda_{01}^+ + \lambda_{01}^- + \lambda_{02}^+ + \lambda_{02}^-)\},$$

with similar expressions for  $Q(q)$  and  $\Lambda(q)$  (not shown here). We also introduce here the shorthand notation  $\lambda_i^\pm = \lambda_i(\mathbf{q}, \pm \omega)$ .

The real part  $\text{Re}\lambda_i(\mathbf{q}, \omega)$  is defined by Eqs. (C1)–(C3), implying that its principal value has been taken for this case. The imaginary part of  $\lambda_i(\mathbf{q}, \omega)$  reads

$$\text{Im} \lambda_i(\mathbf{q}, \omega) = -\frac{\pi}{N} \sum_{\mathbf{p}} n_i(\varepsilon_{i\mathbf{p}}) \delta(\omega - \varepsilon_{i\mathbf{p}} + \varepsilon_{i\mathbf{p}-\mathbf{q}}), \quad (\text{C4})$$

$$\text{Im} \lambda_0(\mathbf{q}, \omega) = -\frac{\pi}{N} \sum_{\mathbf{p}} \delta(\omega - \varepsilon_{1\mathbf{p}} - \varepsilon_{2\mathbf{p}-\mathbf{q}}), \quad (\text{C5})$$

$$\text{Im} \lambda_{0i}(\mathbf{q}, \omega) = -\frac{\pi}{N} \sum_{\mathbf{p}} n_i(\varepsilon_{i\mathbf{p}}) \delta(\omega - \varepsilon_{i\mathbf{p}} + \varepsilon_{j\mathbf{p}-\mathbf{q}}), \quad i \neq j. \quad (\text{C6})$$

The main physics can be captured in a long-wave limit,  $(ak) \ll 1$ , when the spin wave energies possess a quadratic dispersion law, Eqs. (20) and (21). Within this approximation, integration over the angle between the momentums  $\mathbf{p}$  and  $\mathbf{q}$  leads us to an intermediate result for the real parts of (C1)–(C3):

$$\text{Re} \lambda_i(a^\pm) = \frac{1}{2Dq} \int_0^1 n_i(\varepsilon_{i\mathbf{p}}) p dp \ln \left| \frac{p + a^\pm}{p - a^\pm} \right|, \quad (\text{C7})$$

$$\text{Re} \lambda_0(b^\pm) = \frac{1}{2Dq} \int_0^1 p dp \ln \left| \frac{p^2 - pq + b^\pm}{p^2 + pq + b^\pm} \right|, \quad (\text{C8})$$

$$\text{Re} \lambda_{0i}(b^\pm) = \frac{1}{2Dq} \int_0^1 n_i(\varepsilon_{i\mathbf{p}}) p dp \ln \left| \frac{p^2 + pq + b^\pm}{p^2 - pq + b^\pm} \right|, \quad i \neq j. \quad (\text{C9})$$

Here we introduce the parameters  $a^\pm = \frac{q}{2} \pm \frac{\omega}{2Dq}$  and  $b^\pm = \frac{q}{2} + \left[ \frac{q^2}{4} + \frac{(b_1 - b_2)J_0 \pm \omega}{2D} \right]^{1/2}$ . Like for the imaginary parts, we obtain

$$\text{Im } \lambda_i(a^\pm) = \frac{\pi}{2Dq} \int_{|a^\pm|}^1 n_i(\varepsilon_{i\mathbf{p}}) p d p, \quad (\text{C10})$$

$$\text{Im } \lambda_0(b^\pm) = \frac{\pi}{2Dq} \int_{|b^\pm|}^1 p d p = \frac{\pi}{4Dq} [1 - (b^\pm)^2], \quad (\text{C11})$$

$$\text{Im } \lambda_{0i}(b^\pm) = \frac{\pi}{2Dq} \int_{|b^\pm|}^1 n_i(\varepsilon_{i\mathbf{p}}) p d p, \quad i \neq j. \quad (\text{C12})$$

Below we estimate these integrals for the regimes when the parameter  $|a^\pm|$  or  $|b^\pm|$  is small and one can find dominant contributions in expressions (C7)–(C12).

(i)  $|a^\pm| \ll 1$ . If  $|a^\pm|$  is small, which follows from expressions (C7) and (C10), the functions  $\lambda_1^\pm$  and  $\lambda_2^\pm$  give the main contribution. The required asymptotic expansions are found to be

$$\begin{aligned} \text{Re}(\lambda_1^+ + \lambda_1^-) &\approx \frac{T}{D^2 q} \frac{2b_1 b_2}{(b_1 - b_2)^2} \left[ q \arctg \frac{2b_1 b_2}{(b_1 - b_2)^2} - \frac{2b_1 b_2}{3(b_1 - b_2)^2} \left( q^2 + \frac{\omega^2}{D^2 q^2} \right) \right], \\ \text{Re}(\lambda_2^+ + \lambda_2^-) &\approx \frac{T}{D^2 q} \left( \frac{\pi^2}{4} - q \right), \\ \text{Im}(\lambda_1^+ + \lambda_1^-) &\approx \frac{\pi T}{2D^2 q} \frac{2b_1 b_2}{(b_1 - b_2)^2} \left[ \arctg \frac{2b_1 b_2}{(b_1 - b_2)^2} - q \frac{2b_1 b_2}{(b_1 - b_2)^2} \right], \\ \text{Im}(\lambda_2^+ + \lambda_2^-) &\approx \frac{\pi T}{2D^2 q} \left[ 3 - 2q + \frac{1}{4} \left( q^2 + \frac{\omega^2}{D^2 q^2} \right) \right]. \end{aligned}$$

Using these asymptotes, the main contribution to the longitudinal susceptibility takes the form of expression (25), where the characteristic frequencies are determined by Eq. (26).

(ii)  $|b^\pm| \ll 1$ . Now the functions  $\lambda_0^\pm$  and  $\lambda_{0i}^\pm$  give a substantial contribution. In this  $(\omega, \mathbf{q})$  region the denominator, Eq. (18), reads

$$D(\mathbf{q}, \omega_q) \approx 1 - 2J_{\mathbf{q}} \Phi(\mathbf{q}, \omega_q) = 1 + 2J_{\mathbf{q}} \frac{b_1^2 b_2^2}{(b_1 - b_2)^2} (\lambda_0^+ + \lambda_0^- + \lambda_{01}^+ + \lambda_{01}^- + \lambda_{02}^+ + \lambda_{02}^-). \quad (\text{C13})$$

The real parts of the functions  $\lambda_0^\pm$  and  $\lambda_{0i}^\pm$  are equal to

$$\text{Re}(\lambda_0^+ + \lambda_0^-) \approx -3/4D,$$

$$\text{Re}(\lambda_{01}^+ + \lambda_{01}^-) \approx \frac{T}{D^2 q} \left[ q \ln \left( \frac{D + (b_1 - b_2)J_0}{T} \right) - 2 \ln \frac{(b_1 - b_2)J_0}{T} + \frac{(b_1 - b_2)J_0 \pm \omega}{(b_1 - b_2)J_0} \right],$$

$$\text{Re}(\lambda_{02}^+ + \lambda_{02}^-) \approx \frac{T}{D^2 q} \left( \frac{\pi^2}{4} - q \right).$$

For the excitation damping (the pole imaginary part on the mass surface) we have

$$\gamma(q, \Omega_{\text{exc}}) \approx (b_1 - b_2) J_{\mathbf{q}} \frac{2D^2 q}{T} \text{Im}(\lambda_0^+ + \lambda_0^- + \lambda_{01}^+ + \lambda_{01}^- + \lambda_{02}^+ + \lambda_{02}^-).$$

For the imaginary parts (C11) and (C12) with  $\omega = \Omega_{\text{exc}}$ , calculations yield

$$\text{Im } \lambda_0(q, \Omega_{\text{exc}}) \sim \frac{\pi}{2Dq} [1 - \kappa_0^2],$$

$$\text{Im } \lambda_{01}(q, \Omega_{\text{exc}}) \sim \frac{\pi}{2Dq} \frac{T}{D} \ln \left[ \frac{(b_1 - b_2)J_0 + D}{(b_1 - b_2)J_0 + D\kappa_0^2} \right],$$

$$\text{Im } \lambda_{02}(q, \Omega_{\text{exc}}) \sim \frac{\pi}{2Dq} \frac{T}{D} \ln \left\{ \frac{4b_1 b_2}{(b_1 - b_2)^2} \left[ 2 \ln \frac{T}{(b_1 - b_2)J_0} + \frac{\pi^2}{2} + f(T)q \right] \right\},$$

where the functions  $\kappa_0^2$  and  $f(T)$  are determined by the analytical forms (35) and (33), respectively. Summarizing the results, we obtain the characteristic frequencies defined by Eqs. (32) and (34).

- [1] A. Kirilyuk, A. V. Kimel, and T. Rasing, *Rev. Mod. Phys.* **82**, 2731 (2010); *Rep. Prog. Phys.* **76**, 026501 (2013).
- [2] F. Hansteen, A. Kimel, A. Kirilyuk, and T. Rasing, *Phys. Rev. Lett.* **95**, 047402 (2005).
- [3] C. D. Stanciu, F. Hansteen, A. V. Kimel, A. Kirilyuk, A. Tsukamoto, A. Itoh, and T. Rasing, *Phys. Rev. Lett.* **99**, 047601 (2007).
- [4] K. Vahaplar, A. M. Kalashnikova, A. V. Kimel, D. Hinzke, U. Nowak, R. Chantrell, A. Tsukamoto, A. Itoh, A. Kirilyuk, and T. Rasing, *Phys. Rev. Lett.* **103**, 117201 (2009).
- [5] I. Radu, K. Vahaplar, C. Stamm, T. Kachel, N. Pontius, H. A. Dürr, T. A. Ostler, J. Barker, R. F. L. Evans, R. W. Chantrell, A. Tsukamoto, A. Itoh, A. Kirilyuk, T. Rasing, and A. V. Kimel, *Nature (London)* **472**, 205 (2011).
- [6] T. A. Ostler *et al.*, *Nat. Commun.* **3**, 666 (2012).
- [7] C. E. Graves *et al.*, *Nat. Mater.* **12**, 293 (2013).
- [8] V. López-Flores, N. Bergeard, V. Halté, C. Stamm, N. Pontius, M. Hehn, E. Otero, E. Beaurepaire, and C. Boeglin, *Phys. Rev. B* **87**, 214412 (2013).
- [9] S. Alebrand, U. Bierbrauer, M. Hehn, M. Gottwald, O. Schmitt, D. Steil, E. E. Fullerton, S. Mangin, M. Cinchetti, and M. Aeschlimann, *Phys. Rev. B* **89**, 144404 (2014).
- [10] G. Lefkidis, G. P. Zhang, and W. Hübner, *Phys. Rev. Lett.* **103**, 217401 (2009).
- [11] J. Barker, U. Atxitia, T. A. Ostler, O. Hovorka, O. Chubykalo-Fesenko, and R. W. Chantrell, *Sci. Rep.* **3**, 3262 (2013).
- [12] U. Atxitia, O. Chubykalo-Fesenko, J. Walowski, A. Mann, and M. Münzenberg, *Phys. Rev. B* **81**, 174401 (2010).
- [13] U. Atxitia, P. Nieves, and O. Chubykalo-Fesenko, *Phys. Rev. B* **86**, 104414 (2012).
- [14] U. Atxitia, T. Ostler, J. Barker, R. F. L. Evans, R. W. Chantrell, and O. Chubykalo-Fesenko, *Phys. Rev. B* **87**, 224417 (2013).
- [15] S. Wienholdt, D. Hinzke, K. Carva, P. M. Oppeneer, and U. Nowak, *Phys. Rev. B* **88**, 020406(R) (2013).
- [16] J. H. Mentink, J. Hellsvik, D. V. Afanasiev, B. A. Ivanov, A. Kirilyuk, A. V. Kimel, O. Eriksson, M. I. Katsnelson, and Th. Rasing, *Phys. Rev. Lett.* **108**, 057202 (2012).
- [17] V. G. Bar'yakhtar, V. I. Butrim, and B. A. Ivanov, *JETP Lett.* **98**, 289 (2013).
- [18] S. Mathias, C. La-O-Vorakia, P. Grychtol, P. Granitzka, E. Turgut, J. M. Shaw, R. Adam, H. T. Nembach, M. E. Siemens, S. Eich, C. M. Schneider, T. J. Silva, M. Aeschlimann, M. M. Murnane, and H. C. Kapteyn, *Proc. Natl. Acad. Sci. USA* **109**, 4792 (2012).
- [19] V. G. Vaks, A. I. Larkin, and S. A. Pikin, *Zh. Eksp. Teor. Phys.* **53**, 1089 (1967) [*Sov. Phys. JETP* **26**, 647 (1968)].
- [20] S. A. Pikin, *Zh. Eksp. Teor. Phys.* **54**, 1851 (1968) [*Sov. Phys. JETP* **27**, 995 (1968)].
- [21] Yu. A. Izyumov, N. I. Chaschin, and V. Yu. Yushankhai, *Phys. Rev. B* **65**, 214425 (2002).
- [22] Yu. A. Izyumov, F. A. Kassan-Ogly, and Yu. N. Scryabin, *Field Methods in Theory of Ferromagnetism* (Fiziko-Matematicheskaya Literatura, Moscow, 1974) [in Russian].
- [23] V. G. Baryakhtar, V. N. Krivoruchko, and D. A. Yablonskii, *Green Functions in the Theory of Magnetism* (Naukova Dumka, Kiev, 1984) [in Russian].
- [24] Yu. A. Izyumov, M. I. Katsnelson, and Yu. N. Scryabin, *Magnetism of Itinerant Electrons* (Fiziko-Matematicheskaya Literatura, Moscow, 1994) [in Russian].
- [25] Yu. A. Izyumov and Yu. N. Scryabin, *Statistical Mechanics of Magnetically Ordered Systems* (Consultants Bureau, New York, 1988).
- [26] V. N. Krivoruchko, *Low Temp. Phys.* **7**, 662 (1981).
- [27] R. N. Wilcox, *Phys. Rev.* **174**, 624 (1968).
- [28] P. C. Kwok and T. D. Schultz, *J. Phys. C* **2**, 1196 (1969).
- [29] P. Böni, B. Roessli, D. Görlitz, and J. Kötzler, *Phys. Rev. B* **65**, 144434 (2002).
- [30] D. Forster, *Hydrodynamic Fluctuations, Broken Symmetry and Correlation Functions* (Benjamin, MA, London, 1975).
- [31] U. Atxitia and O. Chubykalo-Fesenko, *Phys. Rev. B* **84**, 144414 (2011).
- [32] C. Stamm, T. Kachel, N. Pontius, R. Mitzner, T. Quast, K. Holldack, S. Khan, C. Lupulescu, E. F. Aziz, M. Wiestruk, H. A. Dürr, and W. Eberhardt, *Nat. Mater.* **6**, 740 (2007).
- [33] B. Koopmans, J. J. M. Ruigrok, F. Dalla Longa, and W. J. M. de Jonge, *Phys. Rev. Lett.* **95**, 267207 (2005).
- [34] K. Baberschke, *Phys. Status Solidi B* **245**, 174 (2008).
- [35] V. N. Krivoruchko, *Low Temp. Phys.* **41**, 670 (2015).
- [36] V. N. Krivoruchko, *Low Temp. Phys.* **40**, 42 (2014).